

Design improvements, assembly and testing of the ICRH antenna for W7-X

D.A. Castaño Bardawil^{a,*}, B. Schweer^b, J. Ongena^b, W. Behr^c, K. Crombé^b, G. Czymek^a, X. Han^a, D. Hartmann^d, K.P. Hollfeld^c, J.P. Kallmeyer^d, A. Krämer-Flecken^a, Ch. Linsmeier^a, O. Neubauer^a, D. Nicolai^a, G. Offermanns^c, G. Satheeswaran^a, I. Stepanov^b, M. Van Schoor^b, M. Vervier^c, R. Wolf^d

^a Forschungszentrum Jülich GmbH, Institut für Energie- und Klimaforschung – Plasmaphysik, Partner of the Trilateral Euregio Cluster (TEC), 52425, Jülich, Germany

^b Laboratory for Plasma Physics, Ecole Royale Militaire-Koninklijke Militaire School, 1000, Brussels, Trilateral Euregio Cluster (TEC) Partner, Belgium

^c Forschungszentrum Jülich GmbH, Zentralinstitut für Engineering, Elektronik und Analytik – Engineering und Technologie, Germany

^d Max-Planck-Institut für Plasmaphysik, Wendelsteinstraße 1, D-17491, Greifswald, Germany

ARTICLE INFO

Keywords:

ICRH
Confinement
3-ion
Antenna
Matching
RF

ABSTRACT

The newly developed ICRH antenna system for the stellarator W7-X will be available for Operational Phase 2.1. The design and application of various components in the ICRH system was validated using a prototype of the antenna box with straps. Electromagnetic characteristics were measured and optimized while reconsidering thermal and mechanical aspects. As a result, several components were improved and introduced to the final antenna design. The layout of a new matching system allows operation of the antenna at 25 MHz and 37.5 MHz without the use of additional line stretchers. The refurbished two radio frequency (RF) generators formerly used at TEXTOR comply with new EU safety standards.

1. Introduction

The ion cyclotron resonance heating (ICRH) antenna will be installed for operational phase 2.1 (OP 2.1) at the Wendelstein 7-X (W7X) stellarator. One of its main goals is to allow fast particle confinement studies [1], mimicking fusion-born ⁴He ions in future Helias (HELical Advanced Stellarator) reactors. This is possible by generating fast ions with energies of around 100 keV, since then the fast-ion normalized Lamor-Radius ρ_L/a is about the same for both W7-X and the reactor [2], $(\rho_L/a)_{W7-X} = (\rho_L/a)_{Helias}$, where a is the minor radius of the machine. To generate these fast particles, the antenna will make use of a novel and efficient 3-ion heating technique for multi-ion plasmas [3]. This technique and the particular advantage of ICRH of having no high-density cut-off will also allow additional central heating of high density plasmas [4]. Additionally the system can also be used for ion cyclotron wall conditioning in presence of the stationary magnetic field [1]. For more details and recent developments in physics and technology in the field of ICRH we refer to [4].

The currently developed ICRH [5] system for W7-X is designed to deliver up to 1.5 MW RF power at two resonance frequencies (25 MHz or 37.5 MHz), for pulse duration of 10 s every 5 min. A dedicated

reflectometer is included to assess the influence of ICRH on the edge plasma electron density and for detailed studies on wave-plasma coupling in W7-X [6]. Adapting the radial position of the antenna and providing additional working gas through an injection system should allow to couple efficiently the RF power also to magnetic configurations different from the standard case, for which the antenna shape is optimized (see Figure 23 of reference [1]).

This paper will give an overview of the full ICRH system, presented as follows: (1) ICRH antenna, matching system and RF generators, (2) current assembly status, tests and measurements, and (3) improvements introduced into the design, and (4) conclusions.

2. ICRH antenna, matching system and RF generators

The RF generators and matching system are both located in the ICRH hall. They are connected by underground coaxial transmission lines to the antenna located in the torus hall at the AEE31 port of W7-X as shown in Fig. 1. The matching system adjusts the impedance of the antenna to the output impedance of the RF generators (50 Ω). Coaxial switches allow to direct the RF power to a calorimetric load for calibration purposes and tests, and to operate with one or two generators at a time.

* Corresponding author.

E-mail address: d.castano.bardawil@fz-juelich.de (D.A. Castaño Bardawil).

<https://doi.org/10.1016/j.fusengdes.2020.112205>

Received 14 October 2020; Received in revised form 7 December 2020; Accepted 22 December 2020

0920-3796/© 2021 The Author(s). Published by Elsevier B.V. This is an open access article under the CC BY-NC-ND license

(<http://creativecommons.org/licenses/by-nc-nd/4.0/>).

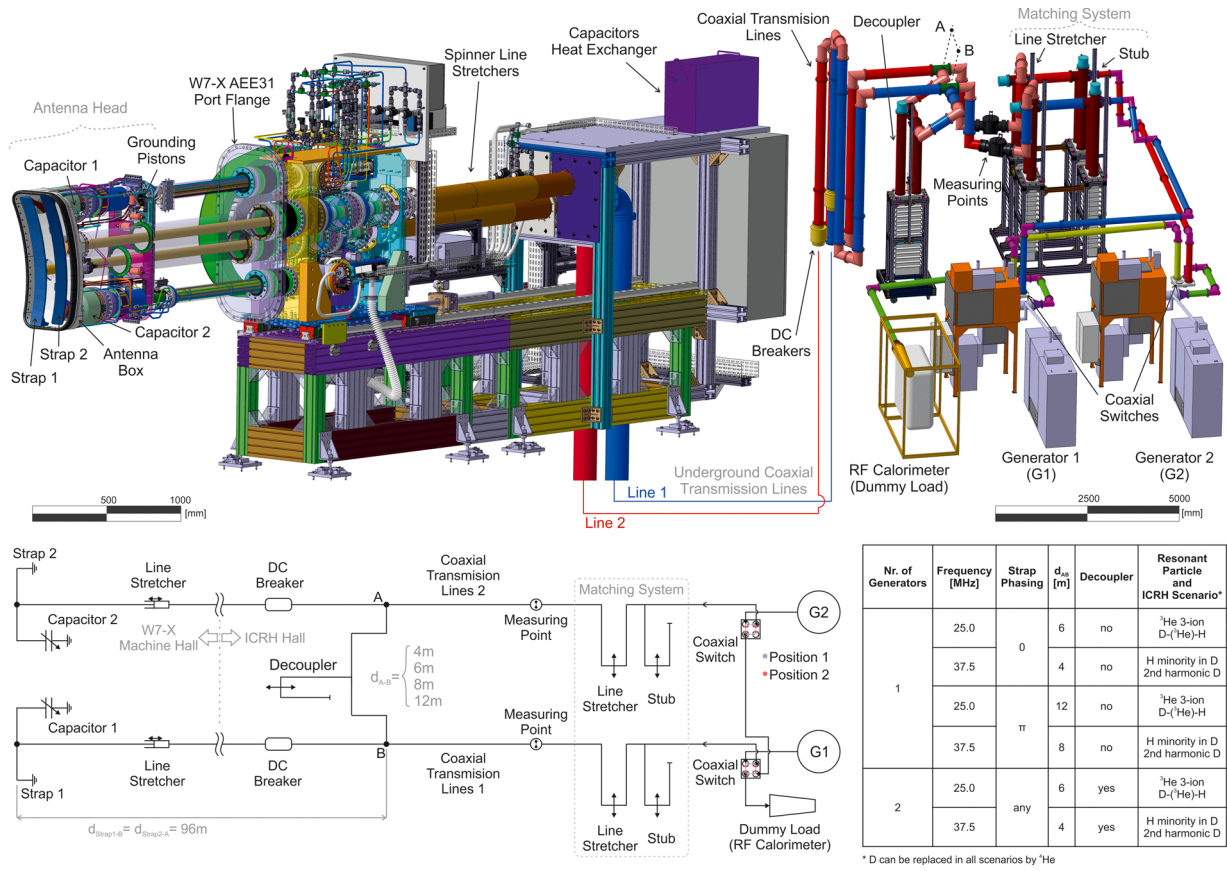


Fig. 1. ICRH System composed of the antenna and the matching generator system. On the bottom left, the electrical concept is shown. On the bottom right, various heating scenarios and corresponding operational parameters are shown.

When operating with two generators, a decoupler is required in addition. This is needed to cancel the RF power flow between the two antenna straps for all antenna phasings different from monopole (0,0) or dipole (0, π), as the RF power flow is proportional to $\sin(\Delta\varphi)$, where $\Delta\varphi$ is the phase difference between the two straps. Pre-matching capacitors are implemented to reduce the voltage on the antenna [7]. During RF operations, the antenna is positioned close to the last closed flux surface. When the antenna is not in use, it is retracted back to its initial parking

position inside the duct.

Data from several locations at the antenna and generator-matching systems are processed and controlled by the SIMATIC process control system from Siemens (PCS7). This is the control and safety standard prescribed for machine operations, auxiliary heating systems and diagnostics at W7-X. For the ICRH antenna system the implementation of control and data acquisition is based on that from the multi-purpose manipulator [8]. Some of the most important parameters to be

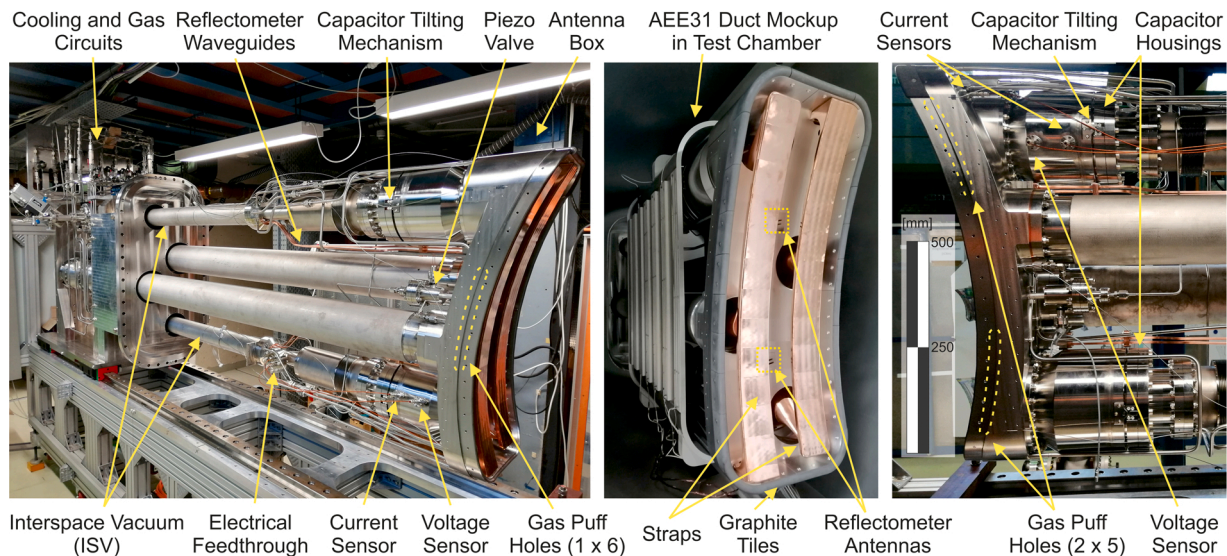


Fig. 2. ICRH Antenna assembled and ready to be introduced into the vacuum chamber for conditioning and testing.

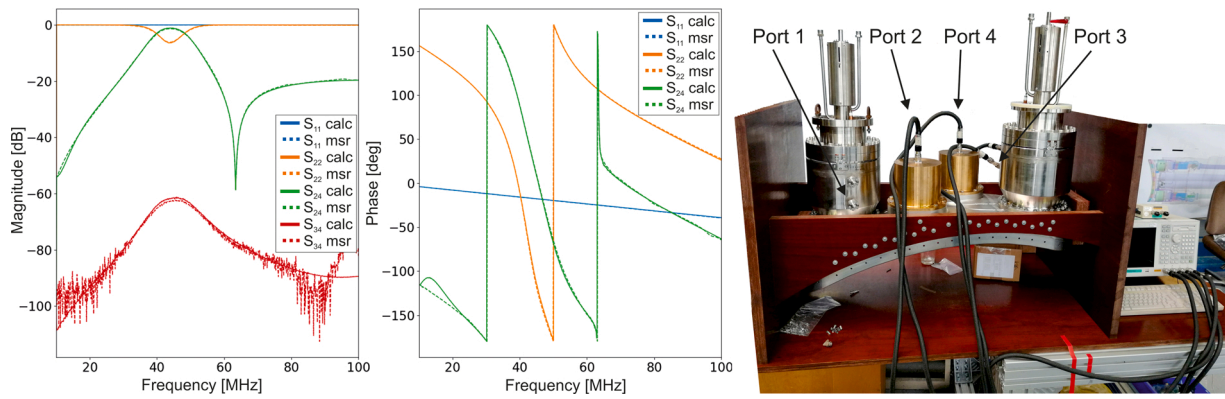


Fig. 3. S-Matrix parameters, magnitude and phase, measured and compared to the calculated values for the antenna box, straps and tuning capacitors. On the right, the setup for measurements (support frame made of wood).

monitored, processed and controlled are: **RF**→ delivered and reflected power, pulse duration, frequency, phasing, current and voltage on antenna straps and pre-matching capacitors; **location and position**→ antenna head in the duct, capacitors setting (pre-matching), line stretcher and stub settings (matching); **temperature**→ cooling water inlet and outlet, antenna head components; **pressure**→ inter space vacuum volumes, grounding pistons, gas puffing system; **flow rate**→ water cooling circuits, gas puffing system.

3. Current assembly status, test and measurements

3.1. ICRH antenna and test chamber

To validate the various components of the antenna system, a purpose-built vacuum chamber has been equipped with a mockup of the W7-X duct that can be heated to simulate the conditions of the AEE31 duct when baking the W7-X device up to 150 °C. A vacuum pressure below 10^{-8} mbar is achieved and needed for the measurement of outgassing and He leakage rates. The vacuum test chamber was also used to perform RF tests (section 3.4) and limit the maximum hydrogen molecule flux to $5 \cdot 10^{20} \text{ s}^{-1}$ at 1 bar and 25 °C for the gas puffing system. Adjusting the flux is possible by changing pulse width modulation of the Piezo valve and by reducing the inlet pressure below 1 bar. Fig. 2 gives an overview of the current status of the ICRH antenna assembly. All water and gas connections have leak rates below $10^{-9} \text{ mbar} \cdot \ell \cdot \text{s}^{-1}$ and are pressure tested up to 40 bar.

3.2. Matching and generator system

Since the use of the RF generators dates back to TEXTOR operations [9], all cabinets required a refurbishment to bring them up to the latest European safety standards. In addition, these systems have been upgraded to communicate with the PCS7 standard. A new matching system layout was designed to allow operation of the antenna at 25 MHz and 37.5 MHz avoiding the use of additional line stretchers. This was achieved by fixing the coaxial transmission line lengths to 96 m, which is a common multiple of the wavelength of the two operational frequencies (12 m and 8 m)

3.3. S-matrix measurements

Measurements of the scattering matrix of the antenna are necessary in order to verify that the antenna has the electrical properties as predicted by the electromagnetic codes during the design phase. Fig. 3 shows some measured and calculated S-matrix parameters, for the system composed of the antenna head (antenna box, straps) and two tuning capacitor units. The figures shown are obtained when both capacitors are at their lowest setting (DC capacitance $\sim 28 \text{ pF}$). Ports 1 and 3 are

the output of the voltage probes on capacitors; ports 2 and 4 are the antenna feeding ports. Good agreement is seen between the calculated and measured curves both in magnitude and phase, except for S34 corresponding to the coupling between the capacitor voltage probe and the feeding port on the opposite side of the antenna. These S34 parameters are too small and below the sensitivity of the network analyzer. Other terms of the S-matrix are omitted for clarity but show similar agreement.

3.4. Testing of the pre-matching capacitors

The test for the pre-matching capacitors (uncooled) mounted to the antenna box and connected to the straps, were made under vacuum conditions at 38 MHz since the maximum voltage can be reached with a lower RF current in the capacitor. The RF power was fed to one strap at a time by tuning the corresponding capacitor while the other strap was not connected (open) and its capacitor was completely detuned. The matching positions were adjusted and verified at low power using a network analyzer. The power and pulse length were slowly increased while monitoring the gas pressure in the test chamber. After several hours of outgassing the maximum rated voltage of 40 kV at the capacitor was obtained with about 60 kW RF power for repetitive pulses of 1 s every 2 min. The same test was repeated for the second strap and corresponding pre-matching capacitor. No evidence of electrical breakdowns was found in the measured signals and by visual inspection at the antenna box and strap surfaces.

4. Improvements introduced to the design

Some antenna components required changes from the thermal, mechanical, electrical, manufacturing, and assembling points of view. This was needed because of differences in the expected heat loads, corresponding thermal expansions and cooling requirements. In addition some components failed during assembly. Two examples are listed below.

4.1. Strap-capacitor connection

The purpose of this connection, consisting of a conical and a flexible component is to:

- allow thermal expansion of the strap and tilting of the capacitors without transferring bending moments, which could generate critical stresses on the capacitor's ceramics;
- to obtain a high electrical conductivity for the RF currents at the surface (skin effect) and
- at the same time to act as a thermal barrier for the heat from the straps keeping the temperature difference between the high voltage

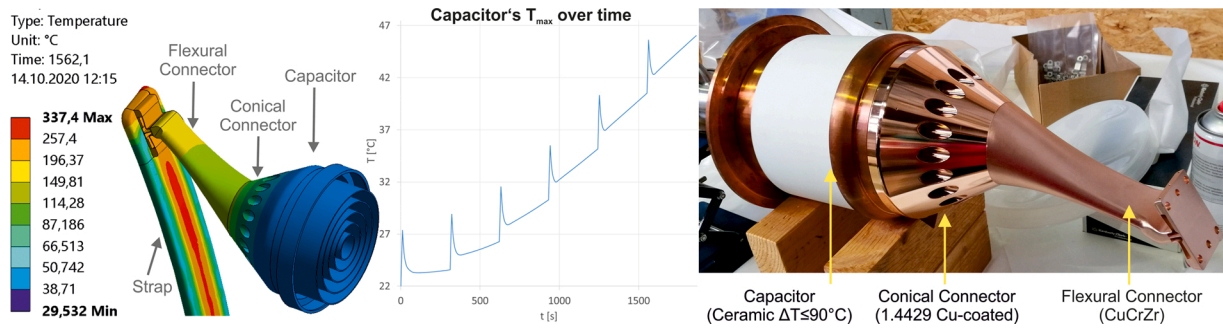


Fig. 4. Transient thermal analyses checking the maximum temperature reached at the capacitor after 6 consecutive RF cycles including absorbed 100 kW/m^2 from the plasma. The photo on the right shows the assembled capacitor unit.

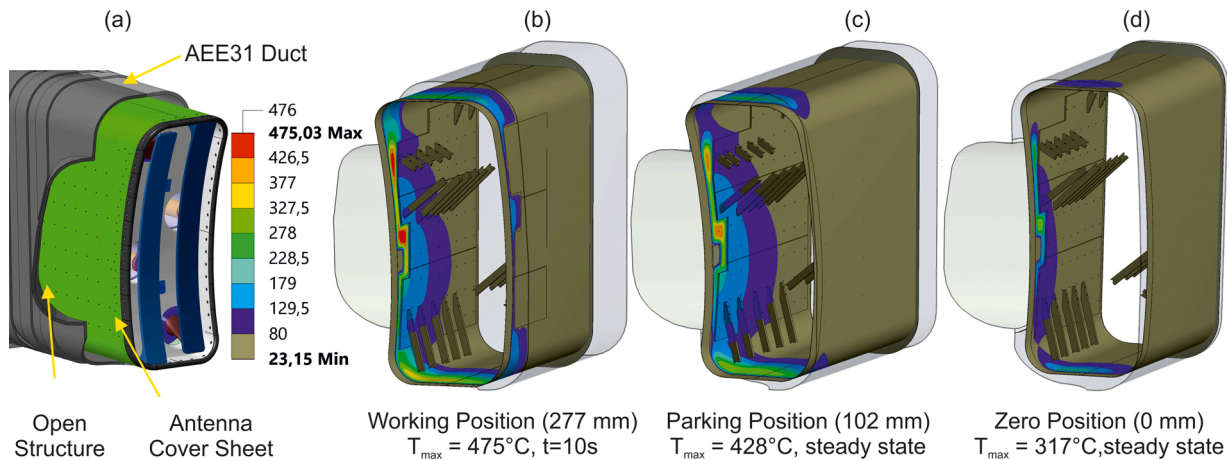


Fig. 5. (a) 3D representation of the analyzed components, (b) transient analysis (10 s, 277 mm) with initial conditions from the steady state parking position results, (c) parking position (antenna aligned to the port lining 102 mm), and (d) steady state thermal analyses for zero position (minimum possible, 0 mm).

and ground side of the ceramic below 90°C (see Fig. 4) during RF operation. This should be valid during 30 min long W7-X pulses, which translates into maximum six consecutive RF cycles (10 s ON, 300 s OFF).

Several combinations of materials and geometries were analyzed in order to realize the most optimal solution. The resulting combination consists in stainless steel (1.4429) with a $20 \mu\text{m}$ copper coating for the conical connector and CuCrZr for the flexible component.

4.2. Cooling of the 1.0 mm antenna cover made of Stainless Steel 1.4429

Due to the open structure next to the antenna (previously foreseen for a neutral beam injector), thermal analyses with a conservative value of absorbed heat flux of 100 kW/m^2 were performed on the cover sheet plate of the antenna head (green structure in Fig. 5a). These analyses showed that during the 10 s RF operation the cover sheet temperature could reach 513°C over a large area. Therefore, additional oxygen-free copper (OF-Cu) cooling plates were attached to the inside of the cover sheet. As a result, the hot area is strongly reduced but the temperature could still become locally about 475°C after RF operation (Fig. 5b). During the 300 s in the parking position, the cover sheet reaches steady state conditions with temperatures up to 428°C (Fig. 5c). However, the antenna is able to move into the duct (if required) over an additional 102 mm, this reduces the local maximum to 317°C (Fig. 5d). To study the variation of the temperature with different heat loads we made calculations assuming 50 kW/m^2 and 30 kW/m^2 with the antenna in the parking position. The resulting maximum steady state local temperatures of the cover sheet become 281°C and 216°C , respectively.

5. Conclusions

The full ICRH antenna concept for W7-X has been presented, including the recently developed matching system, summarizing the efforts made on the design through the previous developing years. Several components were optimized, others newly introduced, while the ones used in the TEXTOR scientific period were refurbished based on the latest European safety standards. A purpose-built vacuum test chamber has been used to validate the functionality, safety, and reliability of preassembled key systems, as well as the fulfillment of all project requirements for commissioning. Very good agreement between measurements and modeling of the system were obtained. With the present schedule, the full ICRH system will be delivered to W7-X in the first half of 2021, in time for commissioning and preparation in OP 2.1. The installed ICRH antenna system would be ready to perform the fast particle confinement studies mimicking fusion-born ^4He ions in future Helias reactors using, among others, the novel and efficient 3-ion heating technique for multi-ion plasmas.

Declaration of Competing Interest

The authors report no declarations of interest.

Acknowledgments

This work has received funding from the Energy Transition Fund from the Belgian Government. It has been carried out within the framework of the EUROfusion Consortium and has received funding from the Euratom research and training programme 2014-2018 and 2019-2020 under grant agreement No 633053. The views and opinions

expressed herein do not necessarily reflect those of the European Commission.

References

- [1] J. Ongena, et al., Study and design of the ion cyclotron resonance heating system for the stellarator Wendelstein 7-X, *Phys. Plasmas* 21 (6) (2014), <https://doi.org/10.1063/1.4884377>.
- [2] M. Drevlak, J. Geiger, P. Helander, Y. Turkin, Fast particle confinement with optimized coil currents in the W7-X stellarator, *Nucl. Eng.* 54 (7) (2014), <https://doi.org/10.1088/0029-5515/54/7/073002>.
- [3] Y.O. Kazakov, et al., Efficient generation of energetic ions in multi-ion plasmas by radio-frequency heating, *Nat. Phys.* 13 (10) (2017) 973–978, <https://doi.org/10.1038/nphys4167>.
- [4] J. Ongena, et al., Recent advances in physics and technology of ion cyclotron resonance heating in view of future fusion reactors, *Plasma Phys. Control. Fusion* 59 (5) (2017), <https://doi.org/10.1088/1361-6587/aa5a62>.
- [5] B. Schweer, et al., Development of an ICRH antenna system at W7-X for plasma heating and wall conditioning, *Fusion Eng. Des.* 123 (2017) 303–308, <https://doi.org/10.1016/j.fusengdes.2017.05.019>.
- [6] X. Han, et al., Development of a Dual-band X-Mode Reflectometer for the Density Profile Measurements at ICRH Antenna in W7-X.pDf [Online]. Available:; Swiss Plasma Cent. Ec. Polytech. Fed. Lausanne Switz. co-operation with Int. At. Energy Agency, 2019 <http://www.aug.ipp.mpg.de/IRW/IRW14/proceedings.html>.
- [7] F. Louche, et al., Three-dimensional modelling and numerical optimisation of the W7-X ICRH antenna, *Fusion Eng. Des.* 96–97 (2015) 508–511, <https://doi.org/10.1016/j.fusengdes.2015.01.039>.
- [8] G. Satheeswaran, et al., A PCS7-based control and safety system for operation of the W7-X Multi-Purpose Manipulator facility, *Fusion Eng. Des.* 123 (2017) 699–702, <https://doi.org/10.1016/j.fusengdes.2017.05.125>.
- [9] TEXTOR Team, et al., Plasma-wall interaction and plasma performance in textor — a review, presented by K.H.Dippel, *J. Nucl. Phys. Mater. Sci. Radiat. Appl.* 145–147 (February) (1987) 3–14, [https://doi.org/10.1016/0022-3115\(87\)90305-9](https://doi.org/10.1016/0022-3115(87)90305-9).